$$I(\sin\theta)=\sin\theta/[\kappa^2+\tfrac{1}{2}U+\tfrac{1}{2}U\sin\theta)^{\frac{1}{2}}+(\kappa^2+\tfrac{1}{2}U-\tfrac{1}{2}U\sin\theta)^{\frac{1}{2}}].$$

From the form of $I(\sin\theta)$, we are able to place the following upper and lower bounds on the change in the zero-point energy

$$\tfrac{1}{2}\sum\delta\omega_n<\left(\frac{L}{2\pi}\right)^2\frac{\pi U^2}{32}[(\kappa^2+U)^{\frac{1}{2}}+\kappa]^{-1}>\left(\frac{L}{2\pi}\right)^2\frac{\pi U^2}{32}\cdot\tfrac{1}{2}(\kappa^2+U/2)^{-\frac{1}{2}}. \qquad \text{(A19)}$$

For $U\gg\kappa^2$, $I(\sin\theta)$ reduces to

$$I(\sin\theta)=(2/U)^{\frac{1}{2}}\sin(\theta/2),$$

which gives

$$\tfrac{1}{2}\sum\delta\omega_n=(L/2\pi)^2(\pi U^{\frac{3}{2}}/32)(0.806). \qquad \text{(A20)}$$

Under this condition, the surface energy per unit area is then approximately

$$(0.806/2^7\pi)U^{\frac{3}{2}}=[(3\alpha^2)^{\frac{3}{2}}(0.806)/2^7\pi]\phi_0{}^3. \qquad \text{(A21)}$$

Since in actual practice ϕ_0 will not have sharp discontinuities, the actual surface energy will be somewhat less than (A21).

PHYSICAL REVIEW VOLUME 88, NUMBER 3 NOVEMBER 1, 1952

The Angular Distribution of Prompt Neutrons Emitted in Fission

J. S. Fraser
Chalk River Laboratory, Atomic Energy of Canada Limited, Chalk River, Ontario, Canada
(Received July 9, 1952)

The angular distribution, relative to the direction of motion of the fragments, of the prompt fast neutrons emitted in the thermal neutron fission of U^{233}, U^{235}, and Pu^{239} has been measured. Collimated fission fragments were selected in energy in a gridded ionization chamber and coincident prompt neutrons in a given direction were counted by proton recoils in an electron collecting chamber filled with methane. The distributions obtained selecting only light fragments have been compared with curves computed on the basis of the evaporation of the neutrons from the moving fragments of the most probable mode. Reasonably good agreement is obtained if one postulates that in the fission of each of the three nuclides studied, the neutron emission probability is about thirty percent greater for the light fragment than for the heavy one. An upper limit of 4×10^{-14} sec following fission may be placed on the time of emission of the neutrons.

I. INTRODUCTION

In 1945, Wilson[1] measured the correlation between the direction of the prompt neutrons and the fragments in the fission process. The results were consistent with the view that the neutrons are evaporated isotropically in the frame of reference of the moving fragments.

The angular dependence of coincidences between fission neutrons has been studied by De Benedetti *et al.*,[2] who concluded that there are twice as many neutron pairs emitted by opposite fragments than by the same fragment.

Prior to the work of Leachman[3] on the ionization yields of fission fragments, it was suggested by Brunton and Hanna[4] that preferential emission of neutrons from one group of fragments may contribute to the disagreement between the distributions in fission fragment mass derived from the ionization and chemical yield measurements. This discrepancy has been shown recently by Leachman[3,5] to be due to a variation in ionization yield with fragment mass and to a dispersion arising from instrumental errors and poor resolution.

The experiment to be described, essentially an extension of Wilson's experiment, was designed to investigate the possibility of preferential emission of neutrons by one of the fragments. It was also found possible to place a much lower limit on the time of emission of the neutrons than the figure of 8×10^{-9} sec given by Snyder and Williams.[6]

II. APPARATUS

A. The Fission Chamber

A cross section of the fission chamber is shown schematically in Fig. 1. A layer of fissile material, approximately 180 μg/cm^2 thick was deposited on a 2.5-cm diameter nickel or aluminum plate which was then cemented to the cathode. Over the source was placed a 0.081-in. thick Dural plate with $\frac{1}{32}$-in. holes drilled in an hexagonal array to act as a collimator. The average angle of emission of the fragments was, therefore, approximately 9° from the normal. The position of the neutron counter was such that the angular uncertainty of the neutron direction was equal to that of the fission fragments passing through the collimator. A

[1] R. R. Wilson, Phys. Rev. **72**, 189 (1947).
[2] De Benedetti, Francis, Preston, and Bonner, Phys. Rev. **74**, 1645 (1948).
[3] R. B. Leachman, Phys. Rev. **83**, 17 (1951).
[4] D. C. Brunton and G. C. Hanna, Can. J. Research **A28**, 190 (1950).
[5] R. B. Leachman, Los Alamos Report LADC 1058 (revised, unpublished).
[6] T. M. Snyder and R. W. Williams, Phys. Rev. **81**, 171 (1951).

Frisch grid of No. 35 B and S copper wires spaced $\frac{1}{16}$ in. apart was used to provide a shielding efficiency of 96 percent.[7] The distance from the source layer to the grid was 2.65 cm; the grid-collector spacing was 0.80 cm. With a gas filling of 1.5 cm of CO_2 and 100-cm argon, saturation of the fission fragment pulses was obtained with a field of 550 volts per cm. A field of 1500 volts per cm between collector and grid was required for zero grid interception. The rise time of the electron collection pulses was about 0.7 μsec. The electrode assembly was mounted in a cylindrical chamber which could be rotated about an eccentric axis through the plane of the fissile layer. A $1\frac{1}{2}$-in. diameter beam of slow neutrons from the thermal column of the *NRX* reactor could thus be made to pass through the source for all angular positions of the chamber.

The U^{233} and U^{235} sources were electrodeposited on nickel disks and the Pu^{239} was put down by the zapon layer technique.[8]

B. The Neutron Counter

In the fission process there are approximately as many γ-rays emitted as there are neutrons. The fast neutron counter in this experiment must therefore be relatively insensitive to these γ-rays. An electron collecting chamber filled to a moderately high pressure with methane fulfills the requirements. The chamber used is shown schematically in Fig. 1. The walls are of $\frac{1}{8}$-in. stainless steel, the end plate being $\frac{1}{2}$ in. thick. The inside diameter is 2.0 in. The 0.040-in. diameter collecting electrode is supported by a $\frac{1}{2}$-in. diameter copper-glass seal and a $\frac{1}{8}$-in. diameter Kovar guard ring. The exposed length of the central electrode is 4.5 in. An earlier model of the chamber included an "O"-ring seal for the endplate. It was found necessary, however, to use welded or soldered joints in order to maintain saturated electron collection over a period of several months. The chamber was heated to about 200°C and pumped for 20 hours before filling. After filling the chamber, the copper pumping tube was pinched off and soldered.

The pressure of the filling, 100 pounds per square inch absolute, was chosen so that the energy lost by a fast electron traversing the length of the counter would be about 200 kev. Since the average fission neutron energy is about 2 Mev, the operating bias could be set to reject most of the γ-ray counts with only a small loss of efficiency for the average neutron. The methane used was of very high purity, prepared at A.E.R.E., Harwell.

The electron collection was tested by measuring the counting rate of Po$-$Be neutrons at a fixed bias as a function of collecting electrode voltage. Throughout the experiment, the saturation curve remained flat from 3500 volts to at least 8500 volts.

[7] Buneman, Cranshaw, and Harvey, Can. J. Research, **A27**, 191 (1949).
[8] B. Rossi and H. Staub, *Ionization Chambers and Counters* (McGraw-Hill Book Company, Inc., New York, 1949), p. 210.

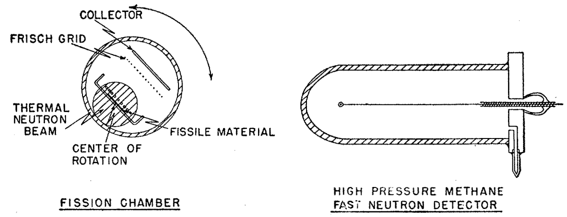

FIG. 1. Schematic diagram of the experimental apparatus.

The variation of neutron counting efficiency with neutron energy was required for the analysis of the experimental results. This was estimated by comparing the methane chamber with a long boron counter using 0.8-Mev neutrons produced by Na^{24} γ-rays on Be, 2.4-Mev neutrons from the D+D reaction, and 14-Mev neutrons from the D+T reaction. The efficiency of the counter at these three energies was (3.25±0.20) percent, (3.26±0.20) percent, and (0.83±0.06) percent, respectively. Between 2.4 Mev and 14 Mev, it was assumed that the efficiency varied as the neutron-proton scattering cross section. The efficiency at 0.8 Mev is approximately one-half of that expected from the variation of the cross section. As the neutron energy is decreased, a greater fraction of the proton recoil pulses are lost below the threshold level of approximately 380 kev. A smooth interpolation of the efficiency curve was made between 2.4 Mev and the threshold energy.

With the bias set at a level corresponding to a proton recoil energy of 380 kev, the counting efficiency for the Na^{24} γ-rays was 0.1 percent of that for the average fission neutron.

C. Electronic Equipment

At the output of the fission pulse linear amplifier, two discriminators were used. The lower one accepted all fission pulses and the upper one those above the valley between the two peaks of the fission fragment energy spectrum. The pulses which triggered the upper discriminator then, are almost entirely due to light fragments entering the chamber. The output pulses from the lower discriminator and from the discriminator on the neutron pulse linear amplifier were fed into a coincidence circuit employing delay line shaped pulses and having a resolving time $2\tau = 2.5$ μsec. The output from the coincidence circuit was fed to a scalar and to a gate circuit which passed the pulse to a second scaler only when the upper fission pulse discriminator was triggered. In this way, the angular distribution of neutron-fragment coincidences was recorded (a) with all fragments selected and (b) with only light fragments. The outputs from the two discriminators on the fission pulse amplifier and from the discriminator on the neutron pulse amplifier were recorded continually on scalers.

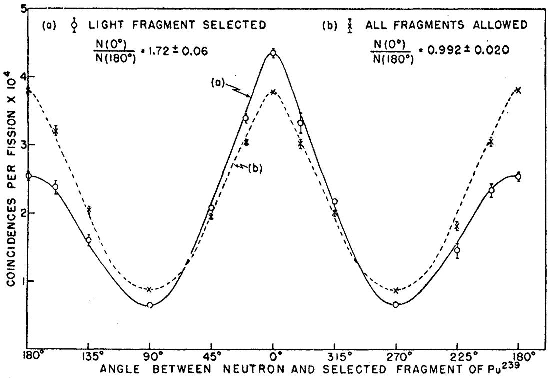

FIG. 2. Experimental prompt neutron angular distribution curves for Pu^{239}.

III. EXPERIMENTAL RESULTS

The first nuclide studied was Pu^{239}. The complete angular distribution curves obtained are shown in Fig. 2. The vertical bars through the points represent the standard errors due to the counting statistics. The solid curve (a) was taken with light fragments only selected. It yields a ratio of the number of coincidences at 0° from the light fragment direction to the number at 180° of 1.72 ± 0.06. 180° from the light fragment corresponds to the direction of motion of the heavy fragment. The dashed curve (b) was obtained with fragments of all energies detected in the fission chamber. For this curve the ratio of the number at 0° to the number at 180° is 0.992 ± 0.020. The symmetry of this curve provides a check on the alignment of the apparatus and demonstrates that there is no measureable difference in the number of neutrons counted per unit solid angle when emitted from a fragment that passes through the gas of the fission chamber and from a fragment that penetrates the source backing.

One would expect no difference between curves (a) and (b) at the 90° and 270° positions. With the neutron counter in a direction perpendicular to the line joining the two fragments, it should be immaterial whether the light or the heavy fragment were detected in the chamber. The source used for these measurements was so non-uniform in thickness that 25 percent of the light fragments were decreased in energy below the upper discriminator level. This, together with the observation that fission modes with low energy light fragments have a greater than average neutron emission probability,[9] may account for the deviation. A subsidiary set of measurements on a uniform source with well-resolved peaks and the same average thickness (190 $\mu g/cm^2$) showed no significant difference in the two curves at 90° and 270°, and the value of the ratio $N(0°)/N(180°)$ was within the stated standard error of that for the first source.

Similar measurements were then made on sources of U^{233} and of uranium enriched to about 15 percent in U^{235}. The results are shown in Figs. 3 and 4 and are similar to those for Pu^{239}. In these figures, the complete angular distribution curves have been folded over the 0°–180° axis and weighted averages taken of the data at corresponding points; the comparison with theory, to be described in Sec. IV, is made only over the 0° to 180° range. In the curves obtained when the light fragments only were selected, values for the ratio $N(0°)/N(180°)$ are 2.05 ± 0.07 and 1.85 ± 0.06, respectively, for the two isotopes.

IV. DISCUSSION

A. Angular Distribution Predicted by the Evaporation Model

The experimental angular distribution may be compared with that calculated on the basis of the following simplifying assumptions: (1) The prompt neutrons are evaporated isotropically in the frame of reference of a moving fission fragment, (2) the neutrons are all emitted in the most probable fission mode, (3) the energy distribution of the neutrons in the frame of reference of a fragment is the same for the light and heavy fragments, and (4) this energy spectrum is the same for the fission fragments of U^{233}, U^{235}, and Pu^{239}.

If η is the energy of a neutron in the fragment's frame of reference, the energy of the same neutron in the laboratory system is[2]

$$E(\eta,\theta)=\eta[1-r^2+2r^2\cos^2\theta \pm 2r\cos\theta(1-r^2+r^2\cos^2\theta)^{\frac{1}{2}}], \quad (1)$$

where θ is the angle between the direction of the fragment and that of the neutron measured in the laboratory system, and r is the ratio of the fragment velocity to the neutron velocity in the fragment's system. The $\pm$ sign applies only when $r>1$ and corresponds to the fact that the neutron may be emitted at either one of two angles in the fragment's system and appear at the same laboratory angle but with different energies E.[10] It can

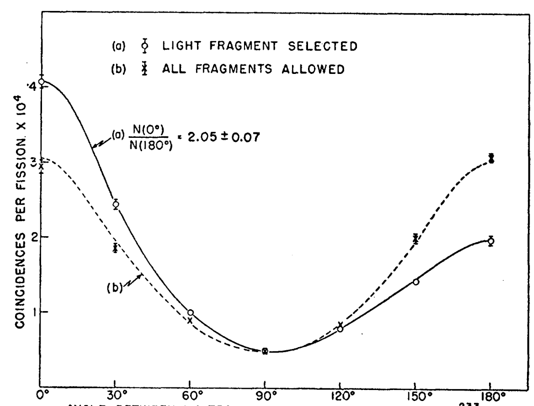

FIG. 3. Experimental prompt neutron angular distribution curves for U^{233}.

[9] J. S. Fraser and J. C. D. Milton (to be published).

[10] N. Feather, BR 335A (unpublished).

be shown that neutrons with the smaller of the two possible energies E make a negligible contribution to the observed angular distribution. For $r\leq 1$, E is single valued.

The probability per unit solid angle that neutrons of emission energy η appear at an angle θ in the laboratory system is[2,11]

$$f(\eta,\theta)=(1/4\pi)(E/\eta)^{\frac{1}{2}}\left|1+r\left[(E/\eta)^{\frac{1}{2}}\cos\theta-r\right]\right|^{-1}. \quad (2)$$

The coincidence counting rate per unit solid angle of neutrons at a laboratory angle θ emitted by a fragment is[2]

$$F(\theta)=\int_0^\infty \phi(\eta)f(\eta,\theta)\epsilon[E(\eta,\theta)]d\eta, \quad (3)$$

where $\phi(\eta)$ is the energy distribution of the neutrons in the fragment's system, and $\epsilon(E)$ is the known efficiency of the neutron counter for neutrons of energy E. If θ is measured from the direction of the light fragment and if R denotes the ratio of the neutron emission probability of the light fragment to that of the heavy, then the angular distribution of coincidences will be given by

$$F(\theta)=\text{const}\times\left\{R\int_0^\infty \phi(\eta)f_L(\eta,\theta)\epsilon_L[E(\eta,\theta)]d\eta + \int_0^\infty \phi(\eta)f_H(\eta,\pi-\theta)\epsilon_H[E(\eta,\pi-\theta)]d\eta\right\}. \quad (4)$$

This equation, with $R=1$, gives that part of the angular distribution which can be ascribed solely to the effects of the motion of the fragments; the asymmetry is expected to vary in the same sense as the ratio of the most probable velocities of the two groups of fragments. Thus, if one knows the form of $\phi(\eta)$, a value for R may be found by fitting the computed angular distribution of neutron-fragment coincidences to the experimental curve.

B. The Emission Spectrum of the Neutrons

The choice of the emission spectrum $\phi(\eta)$ used in this calculation is guided by the fact that it must also give the laboratory energy distribution of fission neutrons, for which the experimental data is available for U^{235}.[12] The laboratory neutron spectrum $\Phi(E)$ given in terms of the emission spectrum, $\phi(\eta)$ is[10]

$$\Phi(E)=\frac{1}{1+R}\left\{\frac{R}{4}\left(\frac{M_L}{mE_L}\right)^{\frac{1}{2}}\int_{\eta_1^L}^{\eta_2^L}\phi(\eta)\eta^{-\frac{1}{2}}d\eta + \frac{1}{4}\left(\frac{M_H}{mE_H}\right)^{\frac{1}{2}}\int_{\eta_1^H}^{\eta_2^H}\phi(\eta)\eta^{-\frac{1}{2}}d\eta\right\}, \quad (5)$$

[11] For example, see L. I. Schiff, *Quantum Mechanics* (McGraw-Hill Book Company, Inc., New York, 1949), first edition, p. 99.
[12] B. E. Watt, AEC Report 3073 (unpublished, 1951).

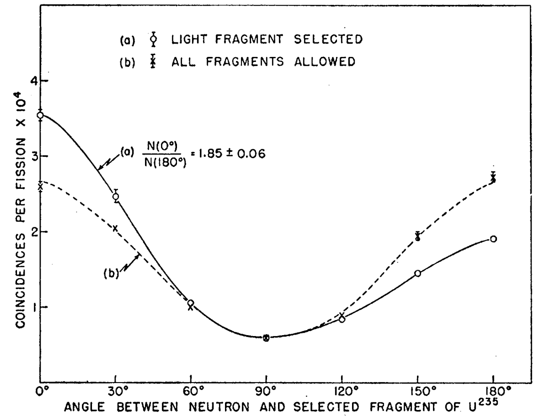

FIG. 4. Experimental prompt neutron angular distribution curves for U^{235}.

where m, M_L, M_H are the masses of the neutron, light, and heavy fragments, respectively, E, E_L, E_H their kinetic energies, respectively, and

$$\eta_1^f=E\left|(mE_f/M_fE)^{\frac{1}{2}}-1\right|^2, \quad \eta_2^f=E\left[(mE_f/M_fE)^{\frac{1}{2}}+1\right]^2. \quad (6)$$

As a first approximation R was set equal to one, since the fitting of $\Phi(E)$ to the experimental data in the energy range below 8 Mev is not very sensitive to small changes in the values of R. It was found, in agreement with Watt,[12] that a good fit could not be obtained with a single "Maxwellian" distribution[10,13] of the form

$$\phi(\eta)=(a\eta/\eta_m)\exp\left[-(a/\eta_m)^{\frac{1}{2}}\eta\right], \quad (7)$$

where a is an exponential level density constant, and η_m the maximum possible neutron energy. This is, however, the distribution predicted by Weisskopf's statistical theory for a nucleus excited sufficiently to emit only one neutron. The number of neutrons emitted in the thermal neutron fission of a U^{235} nucleus is 2.5 ± 0.1,[14] i.e., an average of about 1.25 per fragment. The appropriate theoretical spectrum, therefore, should be that for a nucleus with sufficient internal excitation for the evaporation of between one and two neutrons. This has been given by Feld *et al.*,[15] and in the notation used here is

$$\phi(\eta)=\frac{a\eta}{\eta_m}\exp\left[-\left(\frac{a}{\eta_m}\right)^{\frac{1}{2}}\eta\right]+\frac{a^2\eta}{\eta_m}\int_0^{\eta_m-E_b-\eta} \times\frac{\eta'\exp\left[-\left(\frac{a}{\eta_m}\right)^{\frac{1}{2}}\eta'-\left(\frac{a}{\eta_m-E_b-\eta'}\right)^{\frac{1}{2}}\eta\right]}{\eta_m-E_b-\eta'}d\eta', \quad (8)$$

[13] V. F. Weisskopf, Phys. Rev. **52**, 295 (1937).
[14] Nucleonics **8**, 78 (1951).
[15] Feld, Feshbach, Goldberger, Goldstein, and Weisskopf, AEC Report NYO-636 (unpublished, 1951).

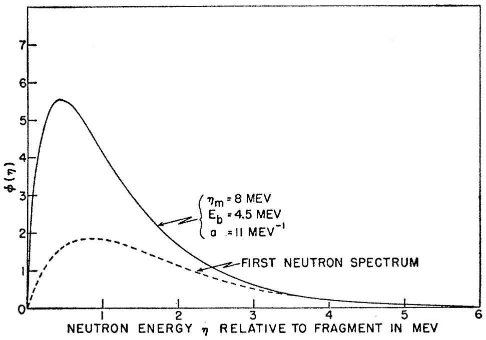

FIG. 5. Calculated prompt neutron emission spectrum for an average primary fission fragment.

where a and η_m are as given in (7), and E_b is the binding energy of the second neutron. The two terms represent the spectrum of "first" and "second" neutrons, respectively. The parameters chosen were $\eta_m=8$ Mev, $E_b=4.5$ Mev for the binding energy of a neutron in an average primary fission fragment, and $a=11$ Mev^{-1} for the exponential level density constant for a medium weight nucleus. The computed emission spectrum $\phi(\eta)$ is shown in Fig. 5 and the comparison of the laboratory energy distribution computed by means of Eq. (5) with the experimental curve given by Watt is shown in Fig. 6. The agreement in the energy range below about 8 Mev is adequate for the present purpose. The contribution to the angular distribution of neutrons whose laboratory energies are greater than 8 Mev is clearly unimportant when the relatively small number involved and decreasing efficiency of the neutron detector with increasing energy are considered. The choice of parameters is not unique. The value of a and E_b are reasonable estimates and $\eta_m=8$ Mev may represent the average value corresponding to a distribution of initial excitation energies. The spectrum given in Fig. 5 was then used in Eq. (4) to compute the angular distribution with the assumption that it is approximately correct for fission fragments of U^{233} and Pu^{239} as well as for those of U^{235}

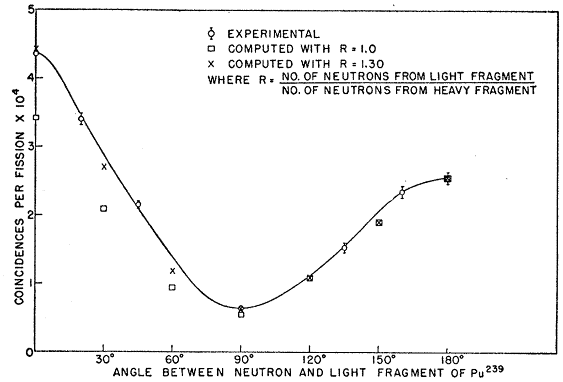

FIG. 7. Comparison of the calculated and the experimental angular distributions of the prompt neutrons in the fission of Pu^{239}.

C. Relative Neutron Emission Probabilities for Light and Heavy Fragments

The result of the calculation for Pu^{239} with $R=1.0$ is indicated by the squares in Fig. 7, the normalization having been done arbitrarily at $\theta=180°$. The points in the region 0° to 90° fall considerably below the experimental curve. The computed curve cannot be brought into agreement with the experimental one by choosing a different spectrum for the neutrons emitted by the light fragment. For example, a spectrum with a lower mean energy than that used would give higher values of $F(\theta)$ near 0°, but lower ones near 90°. The choice of a higher velocity for the light fragment would have a similar effect on $F(\theta)$. A fairly good fit, however, is obtained if one sets $R=1.30$. The curve so obtained is indicated by the x's. It may be concluded, therefore, that the neutron emission probability for the light fragment is on the average about thirty percent greater than that for the heavy fragment. The computed and experimental curves for U^{233} and U^{235} are shown in Figs. 8 and 9; where in both cases a value of $R=1.30$ was found to give a satisfactory fit. The results are summarized in Table I. The ratio V_L/V_H of the most probable velocities for the two fragments is taken from

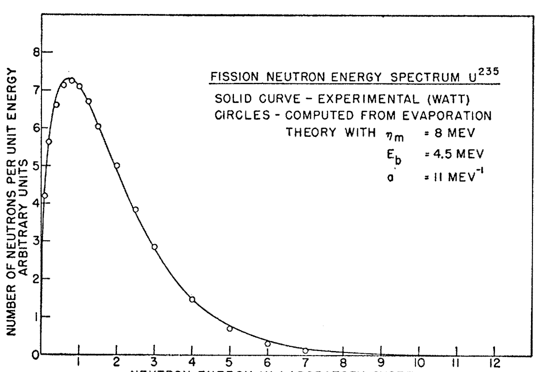

FIG. 6. Comparison of the calculated and the experimental neutron spectrum in the laboratory system for U^{235}.

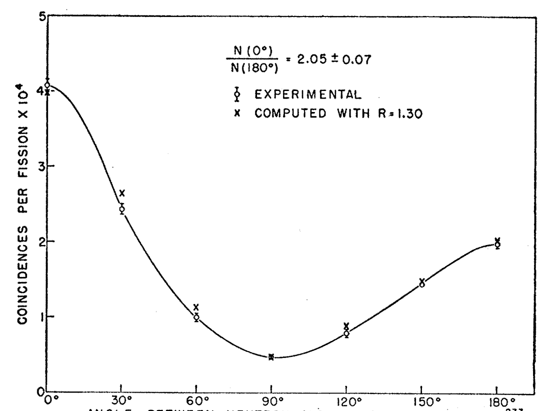

FIG. 8. Comparison of the calculated and the experimental angular distributions of the prompt neutrons in the fission of U^{233}.

Leachman's velocity measurements. The experimental curves have not been corrected for the angular resolution of the apparatus. The part of the curves near 0° where the curvature is greatest would be raised by 5 to 10 percent by such a correction. In view of the limited accuracy of the model used for the calculations, no adjustment in the values of R has been made. The errors stated for R are those in fitting the computed to the experimental curves. It appears that the ratio of neutron emission probabilities for the two fragments is approximately the same for the three nuclides investigated. The trend of the angular distribution towards greater symmetry with increasing mass of the fissile nuclide is evidently associated with the decreasing velocity ratio of the fragments.

D. Time between Fission and the Emission of Neutrons

In Fig. 2 it may be seen that on the dashed curve, representing the angular distribution taken with no energy selection of the fragments, the coincidence rates at the 0° and 180° positions are equal to within 2 percent. The calculated angular distributions discussed in the preceding sections suggest that there is a negligible probability of a neutron being detected in a direction opposite to that of the fragment from which it was emitted. In the 0° position, therefore, the detected neutrons come from fragments entering the gas filling of the chamber, whereas in the 180° position they are from fragments penetrating the aluminum source backing. The number of coincidences at 0° from a fragment may be represented by Eq. (3) with $\theta=0°$. For simplicity suppose that there are ν_f neutrons per fragment all of the average energy $\bar{\eta}$. Then

$$F(0°)=\nu_f f(\bar{\eta}, 0°)\epsilon[E(\bar{\eta}, 0°)]. \qquad (9)$$

If the fragment were to lose a few Mev of kinetic energy before emitting a neutron, the factor in (9) which changes most rapidly is

$$f(\bar{\eta}, 0°)=\frac{1}{4\pi}\left[1+\left(\frac{E_f m}{\bar{\eta} M_f}\right)^{\frac{1}{2}}\right]^2. \qquad (10)$$

TABLE I. Summary of results. V_L/V_H is the ratio of most probable velocities for the two fragments given by Leachman (see reference 6).

Fissile nuclide	$N(0°)/N(180°)$	V_L/V_H	R
U^{233}	2.05±0.07	1.53	1.30±0.08
U^{235}	1.85±0.06	1.47	1.30±0.08
Pu^{239}	1.72±0.06	1.37	1.30±0.08

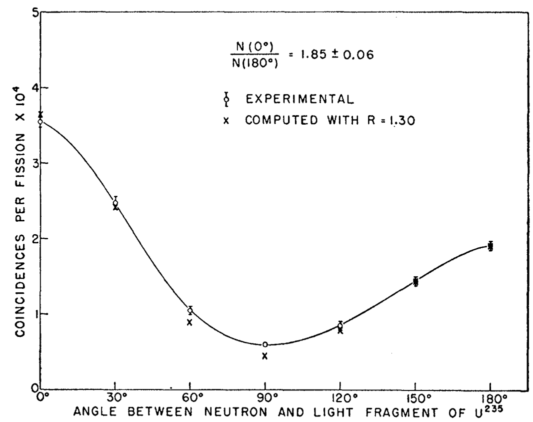

FIG. 9. Comparison of the calculated and the experimental angular distributions of the prompt neutrons in the fission of U^{235}.

A difference in coincidence counting rate of 2 percent, then, in the two positions would correspond to $\delta f/f=0.02$. For $\bar{\eta}=1$ Mev and an average fission fragment, this would occur with a decrease in E_f of $\delta E_f \sim 5$ Mev. The initial specific ionization of an average fission fragment in argon at N.T.P. is about 6 Mev per mm.[16] If one assumes that the initial specific ionization expressed in Mev/(mg/cm^2) in aluminum is related to that of argon as the inverse ratio of the maximum ranges of fission fragments,[17,18] then it follows that the distance traveled in the aluminum by a fragment before it has lost 5 Mev of kinetic energy is about 5×10^{-5} cm. Since the average velocity of a Pu^{239} fission fragment is about 1.2×10^9 cm/sec, the time elapsed in traveling this distance is about 4×10^{-14} sec. It is probable, therefore, that if the time between fission and the emission of prompt neutrons exceeded about 4×10^{-14} sec, the consequent distortions of the prompt neutron angular distribution would have been observed in this experiment.

I wish to express my appreciation to Dr. K. W. Allen (now at the University of Liverpool, Liverpool, England) for valuable discussion in the early stages of this work, to Professor J. D. Jackson of McGill University, Montreal, Quebec, for helpful discussions on the evaporation model, and to Miss M. F. MacGregor and Miss A. R. Rutledge for the numerical computations. The continued interest and encouragement of Mr. G. C. Hanna and of Dr. B. W. Sargent and Dr. L. G. Elliott is gratefully acknowledged.

[16] N. O. Lassen, Phys. Rev. **70**, 577 (1946).
[17] C. Wiegand and E. Segrè, AEC Report MDDC-134 (unpublished).
[18] Flammersfeld, Jensen, and Gentner, Z. Physik **120**, 405 (1943).